Experimental Thermal and Fluid Science 50 (2013) 90–96

Contents lists available at SciVerse ScienceDirect

Experimental Thermal and Fluid Science

journal homepage: www.elsevier.com/locate/etfs

Correlation of turbulent burning velocity for syngas/air mixtures at high pressure up to 1.0 MPa

Jinhua Wang [a,*], Meng Zhang [a], Yongliang Xie [a], Zuohua Huang [a,*], Taku Kudo [b], Hideaki Kobayashi [b]

[a] State Key Laboratory of Multiphase Flow in Power Engineering, Xi'an Jiaotong University, Xi'an 710049, PR China
[b] Institute of Fluid Science, Tohoku University, Sendai, Miyagi 980-8577, Japan

ARTICLE INFO

Article history:
Received 12 March 2013
Received in revised form 23 April 2013
Accepted 17 May 2013
Available online 28 May 2013

Keywords:
Turbulent burning velocity
Syngas
OH-PLIF
High pressure

ABSTRACT

Instantaneous flame front structures of the turbulent premixed flames of syngas/air and CH_4/air mixtures were investigated using OH-PLIF technique at high pressure up to 1.0 MPa, through which the turbulent burning velocities were derived and correlated with the turbulence intensity. Results show that both syngas/air and CH_4/air mixtures, S_T/S_L increases remarkably with the increase of u'/S_L particularly in the weak turbulence region. For the syngas/air mixture, the intensity of flame front wrinkle is promoted with the increase of hydrogen fraction in the syngas due to the increased preferential diffusive-thermal instability. Compared to CH_4/air mixture, the syngas flames possess much wrinkled flame front with much smaller fine cusps structure, and with increasing u'/S_L, the rate of the increase of S_T/S_L for the syngas/air mixtures is more significant than that of CH_4/air mixtures. This demonstrates that the increase of flame front area due to turbulence wrinkling is promoted by flame intrinsic instability for syngas/air mixtures. The values of S_T/S_L for all mixtures increase with the increase of pressure because of the decrease of flame thickness which promotes the hydrodynamic instability. A general correlation of turbulent burning velocity for the syngas/air and CH_4/air mixtures was obtained in the form of $S_T/S_L \propto a[(P/P_0)(u'/S_L)]^n$.

1. Introduction

With ever increasing demand on energy and concerning on environmental protection, the research on the clean alternative power system has attracted an increasing attention. The developed Integrated Gasification Combined Cycle (IGCC) technology based on coal gasification can achieve higher efficiency and lower emissions especially lower CO_2 emission when it combines with Carbon Capture and Storage technology (CCS) [1–3]. The IGCC power plants allow the gasification of wide range of liquid and solid fuel or waste which are converted into the syngas and subsequently consumed in a gas turbine. The main compositions of syngas are CO and H_2. It may also contain small amount of CH_4, N_2, CO_2, H_2O and hydrocarbons [4]. Hydrogen has unique combustion characteristics such as the high reactivity, diffusivity, and the high concentration of free radicals such as O, H and OH in its flames. The existence of small amount of hydrogen has a catalytic effect on CO combustion. However, as hydrogen fraction is increased to a sufficient level, it may cause undesired flame instability issue. Hydrogen possesses fast laminar burning velocity and very thin flame thickness. The increase of pressure results in a significant decrease of flame thickness, which promotes the hydrodynamic instability. Thus the hydrogen fraction in the syngas will induce a quite different turbulence–flame interaction for the turbulent premixed flames in the modern premixed-type gas turbine, compared to that of the traditional hydrocarbon fuels [5].

Meanwhile, the specific composition of syngas depends on the fuel resources and processing condition and has a large variability. Hydrogen mole fractions in syngas varied from 9.0% to 41.4% according to Siemens's report on its IGCC plant fueled with various fuels such as coal, biomass and solid waste [6]. Even in coal based IGCC plant in GE, the hydrogen mole fractions in syngas varied from 25% to 70% depends on the varied processing condition [7]. Variability of syngas composition variability will lead to different turbulence–flame interaction and needs further study in details.

From the practical point of view, turbulent burning velocity is a very important parameter for combustor design and turbulent combustion modeling. A general correlation between turbulent burning velocity and experimental condition is essential [8]. However, due to experimental difficulties, reports on the turbulent burning velocities of syngas/air mixtures at high pressures are very limited. Venkateswaran et al. [9,10] measured the turbulent consumption speeds of syngas/air mixtures and their results indicated a much different sensitivity of turbulent consumption speed to syngas fuel composition. However, the turbulent burning velocity which is a definition dependent quantity was not derived. Chiu et al. [11,12] measured the turbulent burning velocity of syngas

* Corresponding authors. Tel.: +86 29 82665075; fax: +86 29 82668789.
E-mail addresses: jinhuawang@mail.xjtu.edu.cn (J. Wang), zhhuang@mail.xjtu.edu.cn (Z. Huang).

0894-1777/$ - see front matter © 2013 Elsevier Inc. All rights reserved.
http://dx.doi.org/10.1016/j.expthermflusci.2013.05.008

Nomenclature

u'	turbulence intensity, m/s
η_k	Kolmogorov microscale, mm
R_λ	turbulence Reynolds number based on Taylor microscale, mm
S_L	laminar burning velocity, cm/s
Le_{eff}	effective Lewis number
X_i	mole fraction of specific species i
Le_i	Lewis number of specific species i
T_{ad}	adiabatic flame temperature, K
δ_L	flame thickness, mm
L_M	Markstein length, mm
l_i	flame intrinsic instability scale, mm
$\langle c \rangle$	mean progress variable
T_b, T_u	burned and unburned mixture temperature, K
S_T	turbulent burning velocity, cm/s
U	mean velocity of the mixtures at the burner outlet, m/s
θ	angle of the contour $\langle c \rangle = 0.1$
P	pressure, MPa
P_0	environmental pressure, MPa
a	coefficient
n	exponent
S_{LS}	local burning velocity for the stretched flame, cm/s
ε	flame stretch rate, s^{-1}

at high pressure up to 1.2 MPa using a double chamber, high pressure combustion vessel. However, because the pressure in the closed combustion chamber is increasing during the flame propagation process, they could not investigate the turbulent effect at given pressure. Thus the stationary turbulent premixed flames stabilized in a high pressure environment is more suitable to measure the turbulent burning velocity [13]. Turbulent burning velocity and flame front structure of syngas/air mixtures at high pressure up to 1.0 MPa were studied by Ichikawa et al. [5] and Kobayashi et al. [14]. These studies show that the turbulent flame front of syngas/air mixtures is much wrinkled compared to that of CH_4/air mixtures. However, the effect of syngas composition on flame front and turbulent burning velocity was not studied. Thus, the objective of this study is to measure and correlate the turbulent burning velocity of syngas/air mixtures for various syngas compositions at high pressure up to 1.0 MPa. The combined effect of syngas composition and high pressure on flame front structure and turbulence–flame interaction will be examined. A general correlation between turbulent burning velocity and turbulence intensity was obtained for various syngas composition and comparison to that of CH_4/air mixtures is conducted.

2. Experimental setup and procedures

Experiments were performed using the high-pressure combustion test facility at the Institute of Fluid Science, Tohoku University at high pressure up to 1.0 MPa [13]. A brass nozzle-type burner with an outlet diameter of 20 mm was used. Turbulence was generated by a perforated plate installed 40 mm upstream of the outlet. Bunsen-type turbulent premixed flames of $CO/H_2/CO_2$/air mixtures and/or CH_4/air mixtures were stabilized at the burner exit in the high-pressure chamber as shown in Fig. 1, where the ICCD camera is perpendicular to the laser beam. Large amount of fresh air was supplied to the chamber to keep the pressure constant at high pressure and to take away the heat released by the flame. Fuel and air were premixed and supplied to the burner at the temperature of 300 K. Turbulence measurement at high pressure was conducted using a constant-temperature hot-wire anemometer (Dantec, Streamline 90 N) at 300 kHz. Turbulence parameters were calculated by assuming Taylor's hypothesis and isotropic turbulence assumption. Turbulence intensity, u', Kolmogorov scale, η_k, turbulence Reynolds number based on Taylor microscale, R_λ, were shown in Fig. 2. It can be seen that the Kolmogorov scale decreases remarkably with the increase of pressure. Latest direct numerical simulations show that the mean diameter of the vortex of turbulence is about 10 times of the Kolmogorov scale [15]. This indicates that the mean diameter of the vortex of turbulence decreases remarkably with the increase of pressure. More details of the experimental facility and turbulence measurements were presented in Refs. [16,17].

Two syngas compositions were investigated in this study. One is the low caloric syngas with the composition of $XCO/XH_2 = 65/35$ (denoted as CO65). The other is the high caloric syngas with the composition of $XCO/XH_2 = 80/20$ (denoted as CO80). For the syngas/air mixtures, $XCO_2/(XCO + XH_2 + XCO_2)$ is set to be 0.3, reflecting a composition of the syngas. The properties of the mixtures are summarized in Table 1. Laminar burning velocity, S_L, for mixtures used in this study were calculated using the PREMIX code [18] and CHEMKIN-II database [19] with the mechanism by Frassoldati et al. [20] for the syngas/air mixture and GRI-Mech 2.11 [21] for the CH_4/air mixture. Effective Lewis number, Le_{eff}, was evaluated by using the equation, $1/Le_{eff} = (X_1/Le_1 + X_2/Le_2 + \cdots + X_i/Le_i)/(X_1 + X_2 + \cdots X_i)$, where X_i and Le_i are the mole fraction and Lewis number of considered species i [5]. This equation is based on diffusion coefficient of multi-component fuel and oxidizer considering stoichiometry. Thus, for the lean syngas/air mixture, the considered species are CO and H_2. For the stochiometric CH_4/air mixtures, the considered species are CH_4 and O_2. Adiabatic flame temperature, T_{ad}, flame thickness, δ_L, Markstein length, L_M [22], and flame intrinsic instability scale, l_i [23], were also calculated and given in Table 1.

OH-PLIF measurements were performed to visualize the instantaneous flame front. An Nd-YAG laser (Spectra Physics, GCR-250-10) and a DYE laser with a frequency doubler (Spectron, SL4000) were used. A blended branch of Q1(9) and Q2(8) for (1,0) bands of the OH radical was selected for the OH excitation, and almost all OH-LIF emission from the (0,0) band with 308 nm was detected using a high resolution ICCD camera (ANDOR, DH574-18F) with UV lens (Nikkon, UV-105 mm, F4.5 s), a low-pass filter (WG-295), and a broad band-pass filter (UG-5). Thickness of the laser sheet is less than 50 μm and the laser height is about 50 mm at the flame position, and the maximum energy of a single laser shot is about 11 mJ. The OH-PLIF image is 1024 × 1024 pixels and the finest pixel resolution is 0.054 mm/pixel at the measurement plane. More details of the OH-PLIF measurement were stated elsewhere [24,25].

3. Results and discussions

3.1. Flame front structure of syngas/air mixtures for various syngas composition

Fig. 3 shows the turbulent premixed flames of the present work in the Peters modified Borghi diagram [26]. Most of the flames in this study are in the indicated flamelet regime. Thus the flame characteristics can be discussed by applying the flamelet model. The instantaneous flame front OH-PLIF images are shown in

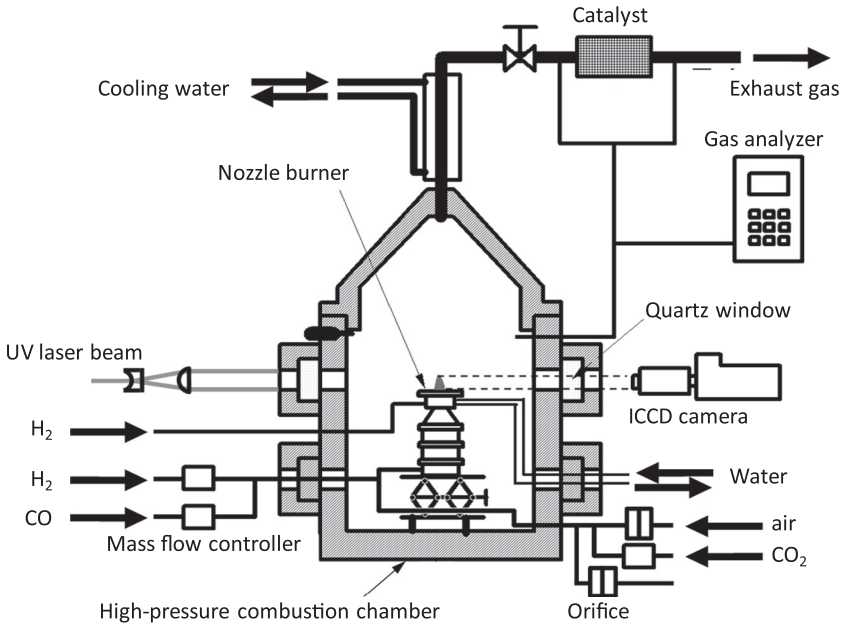

Fig. 1. Schematic of the high-pressure combustion facility [13].

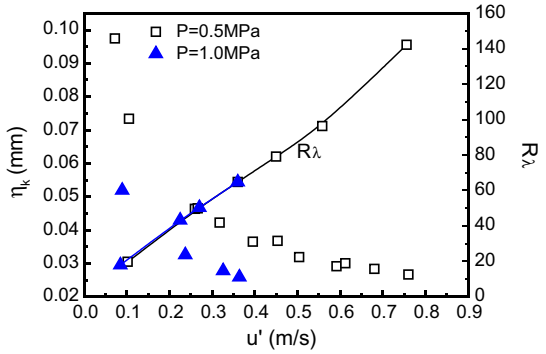

Fig. 2. Kolmogorov scale versus turbulence intensity.

Fig. 4. It can be seen that all the flames in this study possess fine and convoluted flame front structure which is a general characteristic of the turbulent premixed flames at high pressure [16]. The flame front of syngas flames are much finer and wrinkled compared to that of CH_4/air flames and this behavior is much more obvious under low turbulence intensity condition ($u'/S_L \cong 0.55$). Under low turbulence condition, the syngas flames have many fine cusps and these fine cusps with small scale are superimposed on large-scale convex and concave flame wrinkles. While, in the case of CH_4/air flames, large scale flame branches without fine scale cusps are formed and the branches are deep which leads to a thick turbulent flame brush and larger flame volume [5]. With the increase of u'/S_L, the flame height tends to be lower and the flame front tends to be much finer with the decrease of turbulence scale on the wrinkled flame front. It is noted that the difference in flame front structure between the syngas/air and CH_4/air flames tends to be weakened with the increase of u'/S_L. The effective Lewis number of syngas/air mixtures is much less than unity, while that of CH_4/air mixtures are close to unity, as shown in Table 1. This indicates that the flame front structure is significantly influenced by the flame intrinsic instability under the weak turbulence condition [27]. The importance of flame instability on flame front structure is weakened under high turbulence condition, as discussed by Peters et al. [28]. This means that the increase of turbulence is much more effective on wrinkling the flame front, compared to the flame instability. With the increase of hydrogen fraction in syngas, as from CO80 to CO65, the flame height is decreased and flame front tends to be much finer. Many small isolated flame islands appear for CO65 flame at moderate and high turbulence intensities. This might be caused by the significant effect of flame instability on flame front structure with the increase of hydrogen fraction.

The OH-PLIF images of the turbulent premixed flames at pressure of 1.0 MPa are given in Fig. 4b. With the increase of pressure from 0.5 MPa to 1.0 MPa, flame height is decreased and flame front tends to be much finer. This is attributed to the decrease of flame thickness which leads to the promotion of hydrodynamic instability with the increase of pressure. This phenomenon becomes more obvious for the CO65 mixtures under the weak turbulence condition. This indicates that the increase of pressure is more effective for the syngas/air mixtures.

3.2. Turbulent burning velocity measurement and correlation at high pressure up to 1.0 MPa

Fig. 5 gives the progress variable contours $\langle c \rangle$ at 0.1, 0.5 and 0.9. The progress variable c is defined when local temperature is used:

Table 1
Properties of the mixtures in the study.

Mixtures	P (MPa)	ϕ	Lower heating value (kJ/mol)	S_L (cm/s)	T_{ad} (K)	δ_L (mm)	Le_{eff}	L_M (mm)	l_i (mm)
CO65	0.5	0.7	55.6	18.4	1888	0.029	0.60	0.07	0.350
CO80	0.5	0.7	56.9	15.3	1907	0.031	0.72	0.09	0.480
CH_4/air	0.5	1.0	76.1	18.8	2253	0.024	1.05	0.10	0.666
CO65	1.0	0.7	55.6	13.5	1888	0.020	0.60	0.05	0.218
CH_4/air	1.0	1.0	76.1	13.4	2264	0.017	1.05	0.07	0.466

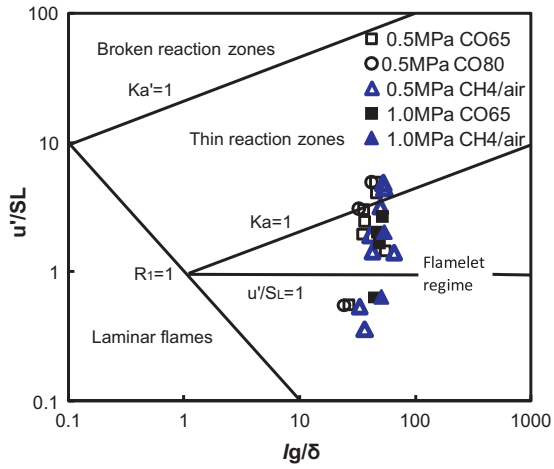

Fig. 3. Borghi's diagram of turbulent premixed flames revised by Peters [26].

$$c(x,y) = [T(x,y) - T_u)]/(T_b - T_u) \quad (1)$$

where T is the local temperature, subscripts u and b represent the unburned and burned mixture temperature, respectively. Flame thickness is sufficiently thin thus it is assumed that $c = 0$ for the unburned mixture and $c = 1$ for the burned mixture. Since OH radical concentration increases quickly at the flame front for the turbulent premixed flame, the binarized images of OH-PLIF are used for the instantaneous boundary between $c = 0$ and $c = 1$. The progress variable contours $\langle c \rangle$ are derived as following. The OH-PLIF instantaneous flame front images are binarized and the flame front curve is derived. About 500 images are averaged to get the progress variable contours $\langle c \rangle$ which indicates the probability of the flame front location of the turbulent premixed flames. In this study, $\langle c \rangle = 0.1$ is considered as unburned side, $\langle c \rangle = 0.5$ is considered as mean flame front location and $\langle c \rangle = 0.9$ is considered as the burned side, respectively. The unburned side $\langle c \rangle = 0.1$ is used to derive the turbulent burning velocity with conventional flame angle method. When the top angle of unburned side, θ, is measured from the contour $\langle c \rangle = 0.1$, the turbulent burning velocity, S_T, is calculated from the following equation:

$$S_T = U \sin(\theta/2) \quad (2)$$

where U is mean velocity of the mixtures at the burner outlet.

The variations of turbulent burning velocity, S_T, with turbulence intensity, u', *and* turbulence Reynolds number based on Taylor microscale, R_λ are shown in Fig. 6. S_T increases linearly with the increase of u' for all mixtures in the experimental range. For CH_4/air mixtures at 0.5 MPa, bending phenomenon between S_T and u' is occurred under high turbulence intensity condition. This bending phenomenon is a general characteristics for the hydrocarbon fuel [27]. However, for CO65 mixtures, no bending phenomenon is observed in the experimental range. This can be explained by the scale model presented by Kobayashi et al. [5,17] that the flame front wrinkled by turbulence vortex is limited to the scale of flame intrinsic instability scale. The S_T for CO65 mixture is larger than that of CH_4/air mixtures under all turbulence conditions even though they possess the same laminar burning velocity. Higher value of S_T of CO65 would be due to the more severely wrinkled flame front structure compared to that of CH_4/air mixtures. As pressure

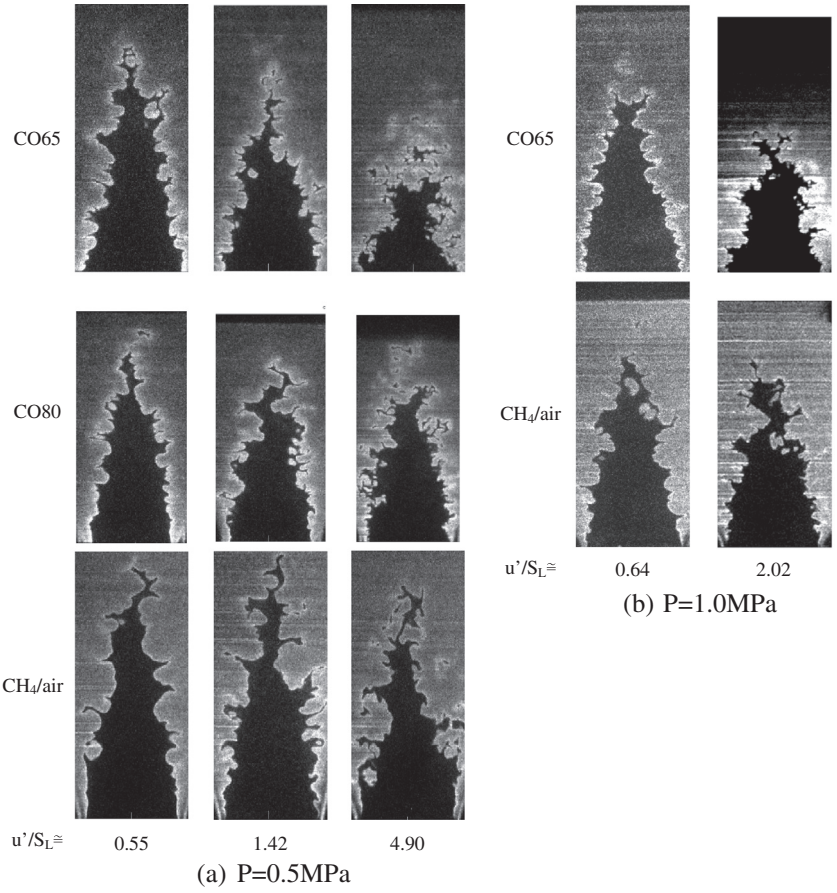

Fig. 4. OH-PLIF images of the turbulent premixed flames under various turbulence conditions: (a) $P = 0.5$ MPa; and (b) $P = 1.0$ MPa.

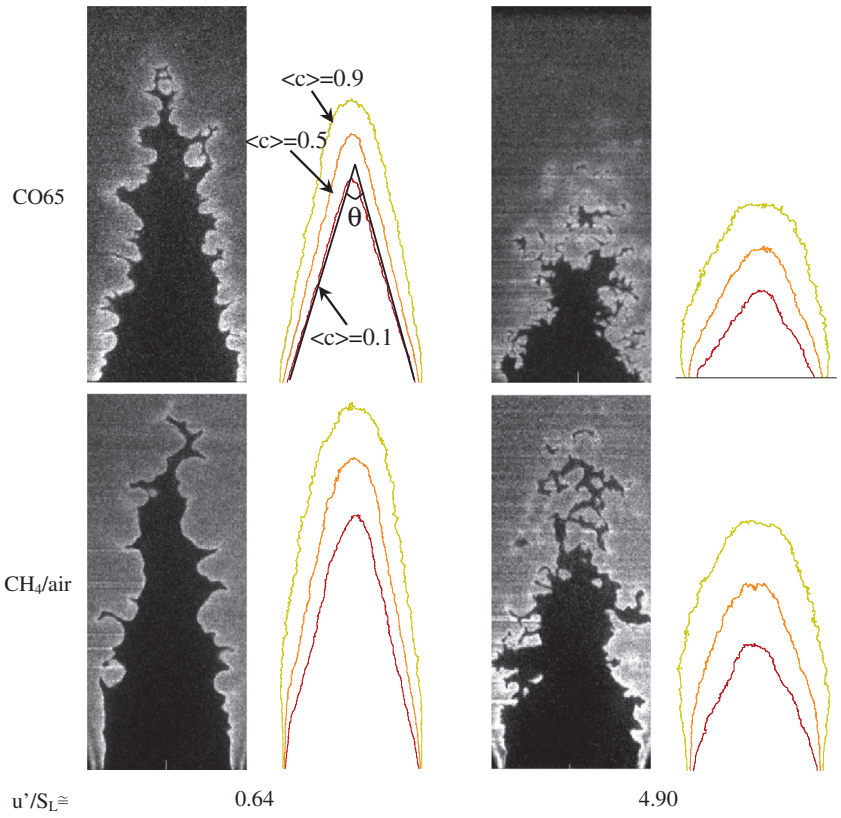

Fig. 5. ⟨c⟩ Contours derived from OH-PLIF images.

increases from 0.5 MPa to 1.0 MPa, the S_T for CO65 mixture increases slightly, while, for that of CH_4/air mixtures decreases slightly compared to CO65. The slight decrease of S_T for CH_4/air mixtures is due to the decrease of laminar burning velocity with the increase of pressure. For CO65 mixtures, the much intensive wrinkled flame front with the increase of pressure compensates the decrease of laminar burning velocity and leads to the slight increase of S_T. This indicates that the effect of high pressure on the increase of S_T is much more obvious for the syngas/air mixtures. The S_T of CO80 is much lower than that of CO65 at 0.5 MPa, and the slope of the fitting line between S_T and u' of CO80 is also slightly lower than that of CO65. The effective Lewis number and intrinsic instability scale of CO80 are larger than CO65 as shown in Table 1 which leads to the different response of flame to turbulence. With the decrease of hydrogen fraction in syngas, the wrinkle of flame front by turbulence vortex is weakened and S_T decreases subsequently. This indicates that the flame intrinsic instability is a dominate factor on the interaction between the turbulence and the flame chemistry. The relationship between S_T and Reynolds number based on Taylor microscale as shown in Fig. 6b is similar to that of turbulence intensity. This indicates that Reynolds number based on Taylor microscale is suitable to represent the turbulence in premixed combustion [24].

Variation of the normalized turbulent burning velocity, S_T/S_L, with u'/S_L is shown in Fig. 7. It is seen that for various hydrogen fraction syngas/air mixture, S_T/S_L increases linearly with the increase of u'/S_L at both 0.5 and 1.0 MPa. While for CH_4/air mixtures, the bending phenomenon between S_T/S_L and u'/S_L is observed for the high turbulence intensity. Additionally, S_T/S_L of CO65 is larger than that of CH_4/air mixtures at 0.5 MPa even though they possess the same S_L, which suggests that the turbulence–flame interaction for CO65 and CH_4/air mixtures is very different. At higher pressures (1.0 MPa), S_T/S_L of CO65 and CH4/air mixtures increases slightly even though S_L decreases substantially. The increase of S_T/S_L for CO65 mixture is much more obvious compared to CH_4/air mixtures with the increase of pressure. S_T/S_L of CO80 is lower than that of CO65, indicating that S_T/S_L decreases remarkably with the decrease of hydrogen fraction in syngas. This is attributed to the effect of preferential diffusive-thermal instability represented by effective Lewis number [29].

In our previous study, a general correlation of S_T/S_L for the CH_4/air mixtures as a power law function of the normalized pressure (P/P_0) and the turbulence intensity (u'/S_L) was proposed [8,24]. In this study, a similar correlation is examined for the syngas/air mixtures under high pressure condition. The correlations of turbulent burning velocity for all mixtures at high pressure are shown in Fig. 8. Generally, a linear correlation of S_T/S_L with $(P/P_0)(u'/S_L)$ based on the logarithmic scale is presented. The small $(P/P_0)(u'/S_L)$ data; however, fail to be linearly correlated. This non-linear phenomenon for low turbulent condition was consistent with the previous study [8,24]. The general correlation of S_T/S_L at 0.5 MPa which masks the small $(P/P_0)(u'/S_L)$ is given in Fig. 8b in the form of:

$$S_T/S_L = a[(P/P_0)(u'/S_L)]^n \tag{3}$$

where the exponent n is close to 0.42 for all the three mixtures in this study, and coefficient a is 3.8, 3.2 and 3.2, respectively for CO65, CO80 and CH_4/air mixtures. Exponent n is in close agreement to our previous study for CH_4/air mixtures, which is close to 0.4, suggesting the unification of the present correlation. The difference on coefficient a would be due to the effect of Markstein length on local burning velocity as shown in Table 1. Markstein length indicates the effect of local stretch on local burning velocity

$$S_{LS} = S_L - \varepsilon L_M \tag{4}$$

where S_{LS} is the local burning velocity for the stretched flame, S_L is the non-stretched laminar burning velocity and ε is the flame stretch rate. For the CH_4/air mixtures at 0.5 MPa, Markstein length is 0.10, and it is 0.07 for CO65. Markstein length of CO80 at

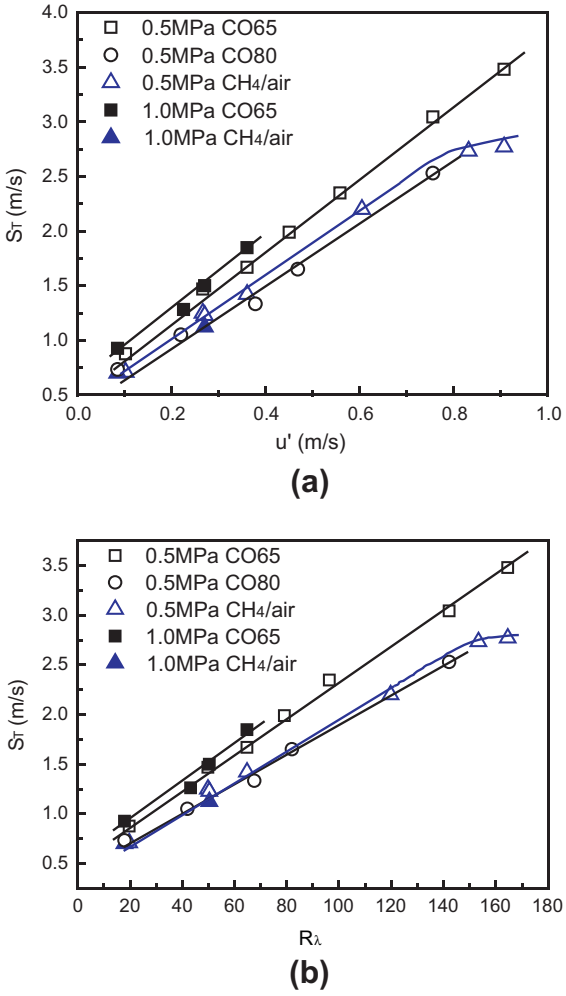

Fig. 6. Relationship between turbulent burning velocity, S_T, turbulence intensity, u', turbulence Reynolds number, R_λ, for various conditions: (a) S_T versus u'; and (b) S_T versus R_λ.

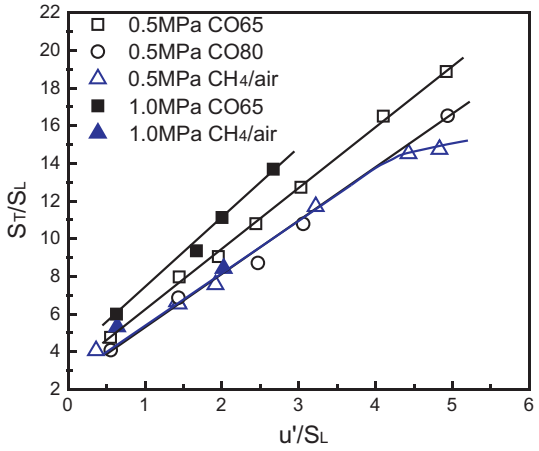

Fig. 7. Relationship between S_T/S_L and u'/S_L for various conditions. Part of the data of CO65 and CH_4/air mixtures are quoted from Ref. [5].

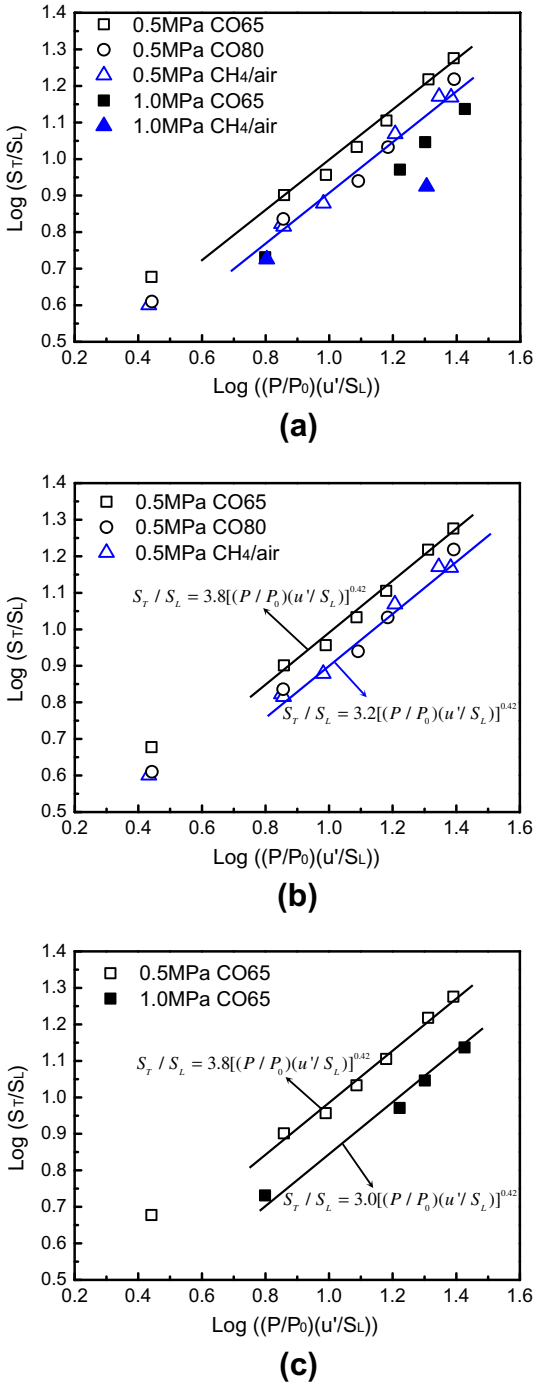

Fig. 8. Correlation of turbulent burning velocity at high pressure of 0.5 MPa and 1.0 MPa: (a) correlation of S_T/S_L for all the mixtures; (b) correlation of S_T/S_L at 0.5 MPa; and (c) correlation of S_T/S_L for CO65 at 0.5 MPa and 1.0 MPa.

0.5 MPa is 0.09 which is close to that of CH_4/air mixtures. When L_M is a large positive value, the local burning velocity decreases with local stretch caused by turbulence vortex motion, leading to the passively response of local turbulent flame front to turbulence vortex motion, and resulting in the larger scale, deep cusps structure for the CH_4/air mixtures, compared to that of syngas/air mixtures as shown in Fig. 4. Larger L_M of CH_4/air and CO80 mixtures leads to the smaller a in the correlation equation compared to that of CO65. The decrease of S_T/S_L with the decrease of hydrogen fraction in syngas is also affected by the effective Lewis number [13]. This indicates that the effect of local stretch on local burning velocity is a predominant factor on the turbulent burning velocity.

Correlation of turbulent burning velocity for CO65 mixture at 0.5 MPa and 1.0 MPa are shown in Fig. 8c. Exponent n remains constant at 0.5 MPa and 1.0 MPa, while, the coefficient a is 3.8 at 0.5 MPa and decreases to 3.0 at 1.0 MPa. The decrease of a with

the increase of pressure is consistent with the previous studies [24,29]. This is because that S_L only decreases slightly with the increase of pressure for a given turbulent intensity, leading to a significant increase of $(P/P_0)(u'/S_L)$ with the increase of pressure. This overestimates the effect of pressure on turbulent burning velocity and leads to the decrease of coefficient a.

4. Conclusions

Measurement and correlation of turbulent burning velocities of syngas/air mixtures for different hydrogen fractions were performed at high pressure up to 1.0 MPa. The following results were obtained:

1. Flame front of turbulent premixed flames at high pressure is a wrinkled flame front with small scale convex and concave structures superimposed with large scale flame branches. The syngas flames possess much wrinkled flame front with much smaller fine cusps structure compared to that of CH_4/air flame. The intensity of flame front wrinkle is promoted with the increase of hydrogen fraction in the syngas.
2. For both syngas/air and CH_4/air mixtures, S_T/S_L increases remarkably with the increase of u'/S_L particularly in the weak turbulence region. The rate of the increase of S_T/S_L for the syngas/air mixtures is higher than that of CH_4/air mixtures. This reflects that the increase of flame front area due to turbulence wrinkling is promoted by flame intrinsic instability for the syngas/air mixtures.
3. S_T/S_L increases with the increase of hydrogen fraction in syngas which can be attributed to the effect of preferential diffusive-thermal instability. S_T/S_L increases with the increase of pressure due to the decrease of flame thickness and subsequently the promotion of hydrodynamic instability.
4. A general correlation of turbulent burning velocity with the pressure and turbulent intensity is obtained.

Acknowledgments

This study is partially supported by National Natural Science Foundation of China (No. 51006080) and the Fundamental Research Funds for the Central Universities. Authors express their thanks to Prof. Yasuhiro Ogami, Dr. Masaki Okuyama and Mr. Futoshi Matsuno at Tohoku University for their helpful and valuable discussion. Jinhua Wang acknowledges the Japan Society for the Promotion of Science for a JSPS postdoctoral Fellowship grant.

References

[1] J.P. Longwell, E.S. Rubin, J. Wilson, Coal: energy for the future, Prog. Energy Combust. Sci. 21 (1995) 269–360.
[2] T.F. Wall, Combustion processes for carbon capture, Proc. Combust. Inst. 31 (2007) 31–47.
[3] B.J.P. Buhre, L.K. Elliott, C.D. Sheng, R.P. Gupta, T.F. Wall, Oxy-fuel combustion technology for coal-fired power generation, Prog. Energy Combust. Sci. 31 (2005) 283–307.
[4] J. Natarajan, Y. Kochar, T. Lieuwen, J. Seitzman, Pressure and preheat dependence of laminar flame speeds of $H_2/CO/CO_2/O_2$/He mixtures, Proc. Combust. Inst. 32 (2009) 1261–1268.
[5] Y. Ichikawa, Y. Otawara, H. Kobayashi, Y. Ogami, T. Kudo, M. Okuyama, S. Kadowaki, Flame structure and radiation characteristics of $CO/H_2/CO_2$/air turbulent premixed flames at high pressure, Proc. Combust. Inst. 33 (2011) 1543–1550.
[6] F. Hannemann, B. Koestlin, G. Zimmermann, G. Haupt, Hydrogen and Syngas Combustion: Pre-Condition for IGCC and ZEIGCC, Siemens AG Power Generation, W8IN, G233.
[7] R.D. Brdar, R.M. Jones, GE IGCC Technology and Experience with Advance Gas Turbines, GE Power Systems, Schenectady, NY, GER-4207.
[8] H. Kobayashi, Y. Kawabata, K. Maruta, Experimental study on general correlation of turbulent burning velocity at high pressure, Proc. Combust. Inst. 27 (1998) 941–948.
[9] P. Venkateswaran, A. Marshall, J. Seitzman, T. Lieuwen, Pressure and fuel effects on turbulent consumption speeds of H_2/CO blends, Proc. Combust. Inst. 34 (2013) 1527–1535.
[10] P. Venkateswaran, A. Marshall, D.H. Shin, D. Noble, J. Seitzman, T. Lieuwen, Measurements and analysis of turbulent consumption speeds of H_2/CO mixtures, Combust. Flame 158 (2011) 1602–1614.
[11] C.C. Liu, S.S. Shy, C.W. Chiu, M.W. Peng, H.J. Chung, Hydrogen/carbon monoxide syngas burning rates measurements in high-pressure quiescent and turbulent environment, Int. J. Hydrogen Energy 36 (2011) 8595–8603.
[12] C.W. Chiu, Y.C. Dong, S.S. Shy, High-pressure hydrogen/carbon monoxide syngas turbulent burning velocities measured at constant turbulent Reynolds numbers, Int. J. Hydrogen Energy 37 (2012) 10935–10946.
[13] H. Kobayashi, Experimental study of high-pressure turbulent premixed flames, Exp. Therm. Fluid Sci. 26 (2002) 375–387.
[14] H. Kobayashi, Y. Otawara, J. Wang, F. Matsuno, Y. Ogami, M. Okuyama, T. Kudo, S. Kadowaki, Turbulent premixed flame characteristics of a $CO/H_2/O_2$ mixture highly diluted with CO_2 in a high-pressure environment, Proc. Combust. Inst. 34 (2013) 1437–1445.
[15] M. Tanahashi, S.J. Kang, T. Miyamoto, S. Shiokawa, T. Miyauchi, Scaling law of fine scale eddies in turbulent channel flows up to Re τ = 800, Int. J. Heat Fluid Flow 25 (2004) 331–340.
[16] H. Kobayashi, T. Nakashima, T. Tamura, K. Maruta, T. Niioka, Turbulence measurements and observations of turbulent premixed flames at elevated pressures up to 3.0 MPa, Combust. Flame 108 (1997) 104–110.
[17] H. Kobayashi, T. Kawahata, K. Seyama, T. Fujimari, J.-S. Kim, Relationship between the smallest scale of flame wrinkles and turbulence characteristics of high-pressure, high-temperature turbulent premixed flames, Proc. Combust. Inst. 29 (2002) 1793–1800.
[18] R.J. Kee, F.M. Rupley, J.A. Miller, A FORTRAN Chemical Kinetics Package for the Analysis of Gas Phase Chemical Kinetics, Report SAND89-8009B, Sandia National Laboratories, Albuquerque, NM, 1993.
[19] R.J. Kee, J.F. Grcar, M.D. Smooke, J.A. Miller, A FORTRAN Program for Modeling Steady Laminar One-Dimensional Premixed Flames, Report SAND85-8240, Sandia National Laboratories, Albuquerque, NM, 1985.
[20] A. Frassoldati, T. Faravelli, E. Ranzi, The ignition, combustion and flame structure of carbon monoxide/hydrogen mixtures. Note 1: detailed kinetic modeling of syngas combustion also in presence of nitrogen compounds, Int. J. Hydrogen Energy 32 (2007) 3471–3485.
[21] C.T. Bowman, R.K. Hanson, D.F. Davidson, W.C. Gardiner, V.L. Jr., G.P. Smith, D.M. Golden, M. Frenklach, M. Goldenberg, GRI-Mech Homepage, 1994, <http://www.me.berkeley.edu/gri_mech/>.
[22] M.J. Brown, I.C. McLean, D.B. Smith, S.C. Taylor, Markstein lengths of CO/H_2/air flames, using expanding spherical flames, Proc. Combust. Inst. 26 (1996) 875–881.
[23] J. Yuan, Y. Ju, C.K. Law, On flame-front instability at elevated pressures, Proc. Combust. Inst. 31 (2007) 1267–1274.
[24] H. Kobayashi, K. Seyama, H. Hagiwara, Y. Ogami, Burning velocity correlation of methane/air turbulent premixed flames at high pressure and high temperature, Proc. Combust. Inst. 30 (2005) 827–834.
[25] H. Kobayashi, H. Hagiwara, H. Kaneko, Y. Ogami, Effects of CO_2 dilution on turbulent premixed flames at high pressure and high temperature, Proc. Combust. Inst. 31 (2007) 1451–1458.
[26] N. Peters, Turbulent Combustion, Cambridge University Press, Cambridge, UK, 2000.
[27] A.N. Lipatnikov, J. Chomiak, Turbulent flame speed and thickness: phenomenology, evaluation, and application in multi-dimensional simulations, Prog. Energy Combust. Sci. 28 (2002) 1–74.
[28] N. Peters, H. Wenzel, F.A. Williams, Modification of the turbulent burning velocity by gas expansion, Proc. Combust. Inst. 28 (2000) 235–243.
[29] S. Daniele, P. Jansohn, J. Mantzaras, K. Boulouchos, Turbulent flame speed for syngas at gas turbine relevant conditions, Proc. Combust. Inst. 33 (2011) 2937–2944.